PERGAMON

International Journal of Solids and Structures 39 (2002) 2557–2574

INTERNATIONAL JOURNAL OF SOLIDS and STRUCTURES

www.elsevier.com/locate/ijsolstr

On the computation of mixed-mode stress intensity factors in functionally graded materials

J.E. Dolbow [a,*], M. Gosz [b]

[a] Department of Civil and Environmental Engineering, Duke University, Box 90287, Durham, NC 27708-0287, USA
[b] Department of Mechanical, Materials and Aerospace Engineering, Illinois Institute of Technology, Chicago, IL 60558, USA

Received 11 April 2001; received in revised form 1 February 2002

Abstract

A new interaction energy integral method for the computation of mixed-mode stress intensity factors at the tips of arbitrarily oriented cracks in functionally graded materials is described. In the method, interaction energy contour integrals are defined and expressed in equivalent domain form. The interaction energy integrals involve products of the actual fields, that arise from solution to the boundary value problem, with known auxiliary fields. The auxiliary stress and displacement fields are chosen to be the asymptotic near-tip fields for a crack in a homogeneous material having the same elastic constants as those found at the crack tip in the functionally graded material. The auxiliary strain fields are obtained from the auxiliary stress fields using the constitutive relation for the functionally graded material. A consequence of our choice for the auxiliary strain field is lack of compatibility which leads to extra terms in the domain integrals that need to be evaluated for the sake of accuracy. The mixed-mode stress intensity factors are obtained from the domain integrals as a post-processing step in the extended finite element method. To assess the accuracy of the method, we consider the benchmark problems of an edge-cracked plate and an angled center crack for specimens with a functional gradient in material properties. Excellent agreement is obtained between the numerical results and the analytical solutions for both stress intensity factors in all cases. All numerical results for the stress intensity factors also exhibit domain independence. The pertinent post-processing routines are provided for download via the world wide web.

Keywords: FGM; Mixed-mode SIFs; Interaction integral; X-FEM

1. Introduction

Advanced material systems are required to withstand highly adverse operating conditions experienced by safety-critical structures such as aircraft fuselages, microelectronic devices, and bio-engineered implants. Functionally graded materials (FGMs) offer the possibility of optimizing system performance through a prescribed tailoring of microstructure and chemistry. For example, functionally graded composite layers formed by varying constituent volume fraction and orientation exhibit substantially better mechanical

* Corresponding author. Tel.: +1-919-660-5202; fax: +1-919-660-5219.
E-mail address: jdolbow@duke.edu (J.E. Dolbow).

0020-7683/02/$ - see front matter
PII: S0020-7683(02)00114-2

response than those fabricated using conventional coating technology (Nadeau and Ferrari, 1999). In contrast to the sharp bimaterial interfaces that commonly arise in traditional systems, the gradual change in material properties throughout an FGM seems to improve their resistance to interfacial delamination and fatigue crack growth (Takahashi et al., 1993). The extent to which material properties can be tailored to guard against specific fracture and failure patterns is presently unknown. Such questions have motivated much of the recent research into the numerical computation of fracture parameters and the simulation of crack growth in FGMs.

For certain classes of FGMs, it has been shown that the asymptotic crack-tip stress and displacement fields have the same form as those in homogeneous materials (Eischen, 1983). The effect of material property variation manifests itself in the near-tip stress intensity factors as well as higher order terms in the asymptotic expansion. An excellent review article on the subject has been written by Erdogan (1995). Although some analytical expressions for stress intensity factors for cracks in FGMs have been derived, investigations have been limited to semi-infinite or infinite domains and simple load cases. Analytical expressions for mixed-mode stress intensity factors have been recently obtained by Gu and Asaro (1997) for cases where the crack tip was oriented perpendicular to the material gradient. A more general case of material gradients with respect to crack orientation was obtained in Konda and Erdogan (1994), albeit for infinite domains. In order to correlate fracture toughness data and to determine critical crack lengths in more general specimens, a numerical method for determining mixed-mode stress intensity factors in FGMs is obviously desirable.

From a numerical perspective, one of the challenges concerns the need for examining the limiting case of a vanishing contour for the proper evaluation of the J-integral (Rice, 1968) for crack tips in FGMs (Honein and Herrmann, 1997). This need stems from the fact that for some in-homogeneous materials and crack tip orientations, the integrand in the J-integral is not divergence free. As a result, an evaluation of the integral on finite contours will exhibit path dependence. To address this issue, Gu et al. (1999) proposed the use of a sufficiently refined mesh near the crack tip, while Anlas et al. (2000) developed a modified path-domain form of the J-integral. While these techniques were successful, the developments are limited to pure mode I problems.

Among the available methods for calculating fracture parameters, the interaction energy integral method (Yau et al., 1980) has emerged as a useful technique for the extraction of mixed-mode stress intensity factors. The contour integrals are derived directly from the J-integral by considering an additive composition of the existing fields with a judicious choice of known auxiliary fields. For the purpose of post-processing finite element solutions, the contour integrals are typically recast as equivalent domain integrals over a finite region surrounding the crack tip. This process removes the need to precisely capture the details of the singular fields near the crack tip, and the approach has been shown to be well suited for a wide class of fracture problems. Nakamura (1991) employed this method to determine mixed-mode stress intensity factors along straight, three-dimensional bimaterial interface cracks. More recently, the same approach has been successfully applied to curved three-dimensional bimaterial interface cracks (Gosz et al., 1998), and through-cracks in Mindlin–Reissner plates (Dolbow et al., 2000b).

In the present paper, we consider the plane problem of an arbitrarily oriented crack in an FGM and present an interaction energy integral method for extracting the mixed-mode stress intensity factors at the crack tips. In the method, interaction energy contour integrals are defined and expressed in equivalent domain form. The formulation is restricted to cracks in linearly elastic, isotropic bodies with smoothly varying elastic moduli. An important step in the derivation of the domain form of the interaction energy integral is the choice of appropriate auxiliary stress, strain, and displacement fields. Here we choose the auxiliary stress and displacement fields to be the familiar asymptotic stress and displacement fields for a crack in a homogeneous material. The elastic constants involved in the auxiliary displacement fields are taken to be the local values found at the crack tip in the functionally graded material. The auxiliary strain fields are obtained from the auxiliary stress fields using the constitutive relation for the functionally graded

material. A consequence of our choice for the auxiliary fields is lack of compatibility between the auxiliary strain and displacement fields. This leads to extra terms in the domain integrals that need to be evaluated for the sake of accuracy. The mixed-mode stress intensity factors are obtained from the domain integrals as a post-processing step in the extended finite element method (X-FEM).

During the review period for this article, our attention was called to an excellent paper by Kim and Paulino (2002) examining various methods to evaluate mixed-mode stress intensity factors in FGMs. The interaction energy integral was not derived or examined in their work, but the method presented in this paper can best be compared to the J_k^*-integrals. Indeed, we recover the J_1^*-integral if the auxiliary fields are taken to be equal to the actual fields from the solution of the boundary value problem. However, the use of interaction energy integrals have several advantages over the J_k^*-integrals for FGMs. In particular, the interaction energy integral does not require the evaluation of strain energy densities along the crack faces (assuming they are traction-free). Another advantage is that the method automatically differentiates between the various stress intensity factors; no examination of the displacement fields along the crack faces is necessary. Given these properties, we suggest that the interaction-energy integrals, in combination with the enriched capabilities of the X-FEM, present an attractive alternative to the current state-of-the-art in this field.

To outline the present paper, the derivation of the interaction energy contour integrals and their associated domain forms is presented in Section 2. Section 3 provides a problem statement for the present fracture analysis of FGMs and a brief description of the X-FEM approximation. In Section 4, we present several numerical examples. In particular, we consider the benchmark problem of an edge-cracked plate with a functional gradient in material properties. Excellent agreement is obtained between the numerical results and the analytical solution. Excellent agreement is also obtained for the case of a plate with an inclined center crack, where the functional gradient affects both mixed-mode stress intensity factors. Importantly, the numerical results for the stress intensity factors are shown to exhibit domain independence. Finally, a summary and some concluding remarks are provided in Section 5. A web-link to a site containing the post-processing routines for evaluation of the domain integrals is also provided.

2. The interaction energy integrals

In this section, we present the methodology for extracting mixed-mode stress intensity factors at the tips of cracks in FGMs. Throughout, we assume that the material is isotropic and that the material properties vary smoothly with position. In addition, we restrict our attention to plane problems and assume small strain kinematics. Throughout, the summation convention is implied and the subscripts take on the values 1–2. A comma denotes partial differentiation with respect to the spatial variables.

We begin by considering a crack as shown in Fig. 1. A local orthogonal coordinate system is defined at the crack tip such that the x_1- and x_2-axes lie parallel and normal to the crack faces respectively. Following Nahta and Moran (1993), the general crack-tip contour integral for the measure L can be written as

$$L = \lim_{\Gamma \to 0} \xi_l \int_\Gamma P_{lj} n_j \, \mathrm{d}\Gamma \tag{1}$$

for a general tensor field $\boldsymbol{P}$. In the above, Γ is a contour surrounding the crack tip, ξ_l are the components of the local crack extension, and n_j are the components of the unit outward normal to Γ. As an example, the energy release rate G can obtained from the general crack-tip integral by letting ξ_l be equal to a unit vector pointing in the x_1-direction and taking P_{lj} to be Eshelby's energy–momentum tensor (Eshelby, 1956);

$$G = \lim_{\Gamma \to 0} \int_\Gamma (W \delta_{1j} - \sigma_{ij} u_{i,1}) n_j \, \mathrm{d}\Gamma \tag{2}$$

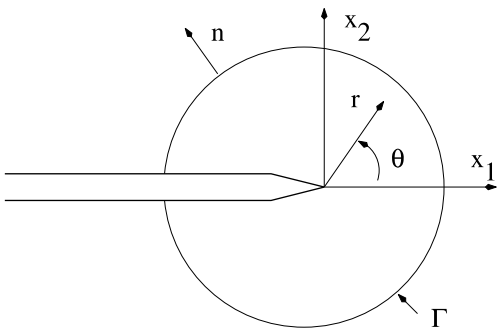

Fig. 1. Contour surrounding a crack tip in a functionally graded material.

where W is the strain energy density, σ_{ij} are the components of the Cauchy stress tensor, and u_i are the displacement components.

2.1. The interaction energy integral

Another crack-tip integral that is useful for extracting the individual stress intensity factors in mixed-mode crack problems is the interaction energy integral. The interaction energy integral is also referred to as the M-integral (see Yau et al., 1980). As its derivation for FGMs is formally similar to that for homogeneous materials, we provide only the key results herein. A detailed derivation can be found in Dolbow et al. (2000a).

We denote the stress σ_{ij}, strain ϵ_{ij}, and displacement u_i fields stemming from the solution of the boundary value problem of interest as the actual fields. We refer to a second set of fields denoted by u_i^{aux}, $\epsilon_{ij}^{\text{aux}}$, and σ_{ij}^{aux} as auxiliary fields, and define them in the next section. The interaction energy integral is obtained by considering the sum of the actual and auxiliary fields in the expression for the energy release rate (2). Through elementary algebraic manipulations, this yields

$$G^{\text{sum}} = G + G^{\text{aux}} + I \tag{3}$$

where G^{aux} is the energy release rate associated with the auxiliary fields, and

$$I = \lim_{\Gamma \to 0} \int_{\Gamma} (\sigma_{ik}\epsilon_{ik}^{\text{aux}}\delta_{1j} - \sigma_{ij}^{\text{aux}}u_{i,1} - \sigma_{ij}u_{i,1}^{\text{aux}})n_j \, \mathrm{d}\Gamma \tag{4}$$

is called the interaction energy integral. For the subsequent developments for FGMs, we call attention to an important assumption in the derivation of I. Namely, the auxiliary stress and strain fields are assumed to be related through the same elasticity tensor $C_{ijkl}(\boldsymbol{x})$ as the actual stress and strain fields, i.e.,

$$\sigma_{ij}^{\text{aux}} = C_{ijkl}(\boldsymbol{x})\epsilon_{kl}^{\text{aux}}; \quad \sigma_{ij} = C_{ijkl}(\boldsymbol{x})\epsilon_{kl} \tag{5}$$

The reason the interaction integral is useful stems from the special relationship between the energy release rate and the stress intensity factors. In the limit as the contour Γ is shrunk onto the crack tip, the contour integral (2) for the energy release rate asymptotes to the following value

$$G = \frac{1}{E_0'}[K_{\text{I}}^2 + K_{\text{II}}^2] \tag{6}$$

where K_{I} and K_{II} are the stress intensity factors associated with the actual fields, and E_0' is defined as

$$E_0' = \begin{cases} E_0 & \text{for plane stress} \\ E_0/(1-\nu_0^2) & \text{for plane strain} \end{cases}$$

Here, E_0 and ν_0 are the local values of Young's modulus and Poisson's ratio at the crack tip.

The analogous relationship for the interaction integral is given by

$$I = \frac{2}{E_0'}[K_{\mathrm{I}}K_{\mathrm{I}}^{\mathrm{aux}} + K_{\mathrm{II}}K_{\mathrm{II}}^{\mathrm{aux}}] \tag{7}$$

The stress intensity factors K_{I} and K_{II} associated with the actual fields can therefore be obtained through a judicious choice of the auxiliary fields. For example, if we choose the auxiliary fields such that $K_{\mathrm{I}}^{\mathrm{aux}} = 1$, and $K_{\mathrm{II}}^{\mathrm{aux}} = 0$, we have

$$K_{\mathrm{I}} = \frac{E_0'}{2} I \tag{8}$$

The mode II stress intensity factor is determined in a similar fashion. The interaction integral therefore provides a straightforward means for decoupling K_{I} and K_{II} in a general mixed mode problem.

2.2. Choice of auxiliary fields

In order to evaluate the interaction energy integral defined in the previous section, it is advantageous for computational purposes to convert the contour integral into an area integral. In order to derive the area integral, we must first, however, define appropriate auxiliary fields. In the present paper where it is desired to obtain the mixed-mode stress intensity factors for crack problems in FGMs, we choose the auxiliary fields in such a manner so as to make the computation of the resulting area integrals as simple as possible. To this end, we choose the auxiliary stress and displacement fields as follows:

$$u_i^{\mathrm{aux}} = \frac{K_{\mathrm{I}}^{\mathrm{aux}}}{2\mu_0}\sqrt{\frac{r}{2\pi}}u_i^{\mathrm{I}}(\theta) + \frac{K_{\mathrm{II}}^{\mathrm{aux}}}{2\mu_0}\sqrt{\frac{r}{2\pi}}u_i^{\mathrm{II}}(\theta) \tag{9}$$

$$\sigma_{ij}^{\mathrm{aux}} = \frac{K_{\mathrm{I}}^{\mathrm{aux}}}{\sqrt{2\pi r}}\sigma_{ij}^{\mathrm{I}}(\theta) + \frac{K_{\mathrm{II}}^{\mathrm{aux}}}{\sqrt{2\pi r}}\sigma_{ij}^{\mathrm{II}}(\theta) \tag{10}$$

The fields defined by Eqs. (9) and (10) are the well known near-tip displacement and stress fields for cracks in homogeneous solids. Here μ_0 is the local value of the shear modulus at the crack tip, and r and θ are the polar coordinates depicted in Fig. 1. The auxiliary strain field is chosen such that

$$\epsilon_{ij}^{\mathrm{aux}} = S_{ijkl}(\boldsymbol{x})\sigma_{kl}^{\mathrm{aux}} \tag{11}$$

where $S_{ijkl}(\boldsymbol{x})$ is the compliance tensor of the functionally graded material.

It is important to recognize that in the definitions (9)–(11) of the auxiliary fields, the auxiliary stress fields are in equilibrium; however, the auxiliary strain fields are not compatible with the auxiliary displacement field. While the terms that give rise to a lack of compatibility are not sufficiently singular in the asymptotic limit to contribute to the value of the interaction energy integral (7), it is important not to neglect these terms in the evaluation of the equivalent area integrals. This is because the auxiliary fields are not just defined asymptotically close to the crack tip but are extended into the domain. Very similar issues have been borne out in the development of the interaction energy integral for other problems in fracture mechanics (see Nahta and Moran, 1993; Gosz et al., 1998; Dolbow et al., 2000b).

There are other suitable choices for the auxiliary fields for extraction of stress intensity factors in FGMs. A seemingly more natural choice of auxiliary fields would be to define the auxiliary displacement fields according to Eq. (9) and then to choose a compatible auxiliary strain field from the symmetric gradient of

the auxiliary displacement field. The auxiliary stress fields would then be defined as $\sigma_{ij}^{\text{aux}} = C_{ijkl}(\boldsymbol{x})\epsilon_{kl}^{\text{aux}}$ in accordance with the constitutive law for the functionally graded material. This choice for the auxiliary stress field, however, would not generally be in equilibrium, and additional terms would also arise in the domain integrals. To see this, we recall that the equilibrium equations in the absence of body forces read $\sigma_{ij,j} = 0$. Substituting in a compatible set of strain fields, and performing some additional manipulations yields

$$\sigma_{ij,j}^{\text{aux}} = C_{ijkl}(0)\epsilon_{kl,j}^{\text{aux}} + C_{ijkl,j}(\boldsymbol{x})\epsilon_{kl}^{\text{aux}} + \big(C_{ijkl}(\boldsymbol{x}) - C_{ijkl}(0)\big)\epsilon_{kl,j}^{\text{aux}}$$

The first term above is identical to the homogeneous fields, and clearly vanishes to satisfy equilibrium. Although some particular choices for the constitutive tensor $\boldsymbol{C}$ may result in the remaining terms also vanishing, it is not difficult to argue that this would not hold in general.

Yet another choice would be to use purely homogeneous auxiliary fields, employing a constant constitutive tensor such that (5) would no longer hold. The additional terms that arise in the domain integrals from this choice of auxiliary fields would involve gradients of the actual stress fields. Given the present context of a $C^0(\Omega)$ finite element approximation for the displacement field, this approach would be fairly intractable. By contrast, the present approach only involves higher order gradients of the auxiliary fields. In view of these arguments, we contend that the definitions (9)–(11) represent the best choice for the auxiliary fields.

2.3. Domain form of the interaction energy integral

We now describe the process of converting the interaction energy contour integral into an equivalent area integral. Assuming for simplicity that the crack faces are traction free, the contour integral (4) can be rewritten as

$$I = -\oint_C P_{1j} m_j q \, \mathrm{d}C \tag{12}$$

where

$$P_{1j} = (\sigma_{ik}\epsilon_{ik}^{\text{aux}}\delta_{1j} - \sigma_{ij}u_{i,1}^{\text{aux}} - \sigma_{ij}^{\text{aux}}u_{i,1}) \tag{13}$$

and $C = C_0 + C_+ + C_- + \Gamma$ is the closed contour defined in Fig. 2, m_j are the components of the unit outward normal to the contour, and q is a test function. We note that the portions of the contour C_+ and C_- coincide with the upper and lower crack faces, and that $m_j = -n_j$ on Γ. The area enclosed by the contour is labeled A in the figure. The weight function $q = q(\boldsymbol{x})$ is defined to be sufficiently smooth in A and takes on the following values on the boundaries of A:

$$q = \begin{cases} 0 & \text{on } C_0 \\ 1 & \text{on } \Gamma \end{cases} \tag{14}$$

Although there are a number of choices for the function q that satisfy the above criteria, the numerical calculations are relatively insensitive as explored in Shih et al. (1986). Next, employing the divergence theorem and taking the limit as the contour gamma is shrunk onto the crack tip, we obtain

$$I = -\int_\Omega P_{1j} q_{,j} \, \mathrm{d}\Omega - \int_\Omega P_{1j,j} \, q \, \mathrm{d}\Omega \tag{15}$$

where Ω is the area enclosed by the contour C_0.

Because of the way in which we have defined the auxiliary fields as explained in the previous section, the auxiliary strain field is incompatible. Therefore, for an FGM the tensor $\boldsymbol{P}$ defined by Eq. (13) is not divergence free and the second integral above does not vanish. This is in marked contrast to the derivation of

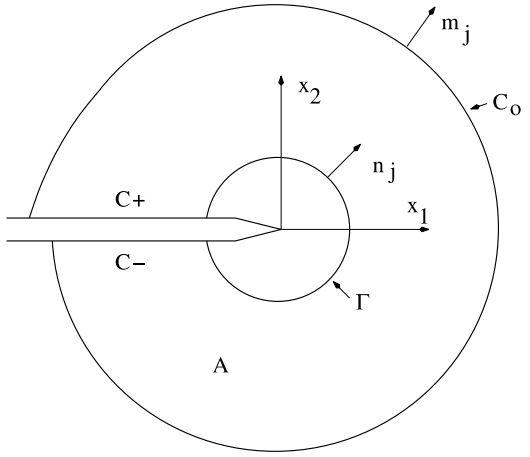

Fig. 2. Conventions at crack tip. Domain A is enclosed by Γ, C_+, C_-, and C_0. Unit normal $m_j = -n_j$ on Γ.

the domain form of the interaction energy integral for homogeneous materials, for which the tensor $\boldsymbol{P}$ is divergence free. Through some algebraic manipulation and the use of the definition (13), the domain form of the interaction energy integral is finally written as

$$I = \int_\Omega (\sigma_{ij} u^{\text{aux}}_{i,1} + \sigma^{\text{aux}}_{ij} u_{i,1} - \sigma_{ik} \epsilon^{\text{aux}}_{ik} \delta_{1j}) q_{,j} \, \mathrm{d}\Omega + \int_\Omega \left[\sigma_{ij} (u^{\text{aux}}_{i,1j} - \epsilon^{\text{aux}}_{ij,1}) \right] q \, \mathrm{d}\Omega - \int_\Omega \left[C_{ijkl,1} \, \epsilon_{kl} \epsilon^{\text{aux}}_{ij} \right] q \, \mathrm{d}\Omega \tag{16}$$

We note that the second integral on the right hand side of the above arises due to the lack of compatibility of the auxiliary strain field. The last integral on the right hand side arises because the elasticity tensor varies with position in FGMs.

We close this section by remarking that when the auxiliary fields are taken to be equal to the actual fields, the equivalent domain form of the J-integral can be obtained:

$$J = \int_\Omega (\sigma_{ij} u_{i,1} - W \delta_{1j}) q_{,j} \, \mathrm{d}\Omega - \int_\Omega \left(\frac{1}{2} \epsilon_{ij} C_{ijkl,1} \, \epsilon_{kl} \right) q \, \mathrm{d}\Omega \tag{17}$$

The above is equivalent to the energy release rate as defined by (2), and also to the stress intensity factors as defined in (6). The same expression can be found in Anlas et al. (2000). We note, however, that the additional terms employed in the contour form of the modified J-integral by Anlas et al. (2000) are in fact unnecessary when deriving equivalent domain integrals, precisely because the contour Γ is shrunk onto the crack tip.

3. Problem formulation

3.1. Problem statement

We consider the fractured body shown in Fig. 3 and assume planar deformations, allowing for a two-dimensional representation of the domain $\Omega \subset \mathscr{R}^2$ bounded by Γ. The boundary Γ consists of the disjoint sets Γ_{u}, Γ_{t}, and Γ_{c}, such that $\Gamma = \Gamma_{\text{u}} \cup \Gamma_{\text{t}} \cup \Gamma_{\text{c}}$. Displacements are prescribed on Γ_{u}, while tractions $\bar{\boldsymbol{t}}$ are imposed on Γ_{t}. In the present investigation, we also assume that the crack faces are traction free.

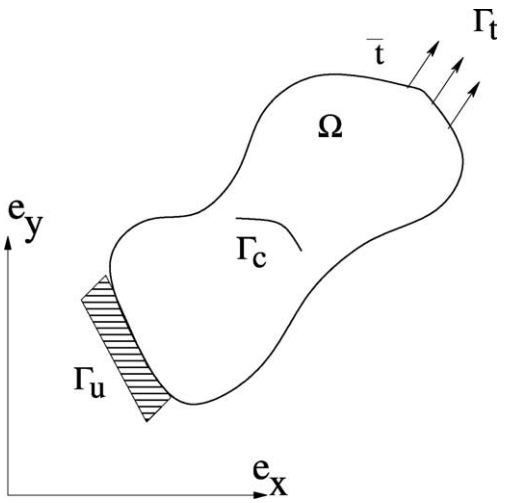

Fig. 3. An FGM with a crack subjected to loads.

We now describe the variational boundary value problem of interest. The space of admissible displacement fields is defined by

$$\mathscr{U} = \{\boldsymbol{v} \in \mathscr{V} : \boldsymbol{v} = \bar{\boldsymbol{u}} \text{ on } \Gamma_u\} \tag{18}$$

where the space $\mathscr{V}$ is related to the regularity of the solution. The test function space is defined similarly as

$$\mathscr{U}_0 = \{\boldsymbol{v} \in \mathscr{V} : \boldsymbol{v} = 0 \text{ on } \Gamma_u\} \tag{19}$$

In the absence of body forces, the problem is to find the displacement field $\boldsymbol{u} \in \mathscr{U}$ such that

$$\int_\Omega \boldsymbol{\epsilon}(\boldsymbol{u}) : \boldsymbol{C} : \boldsymbol{\epsilon}(\boldsymbol{v}) \, d\Omega = \int_{\Gamma_t} \bar{\boldsymbol{t}} \cdot \boldsymbol{v} \, d\Gamma \quad \forall \boldsymbol{v} \in \mathscr{U}_0 \tag{20}$$

In the above, $\boldsymbol{\epsilon}$ is the strain field and $\boldsymbol{C}$ is the fourth order elasticity tensor. We will assume that the material is isotropic, and moreover that the Young's modulus $E(x) \in C^1(\Omega)$ and Poisson's ratio $v(x) \in C^1(\Omega)$ describe the character of the FGM.

3.2. Discretization with the X-FEM

We now briefly describe the extended finite element approximation to (20). The present application is similar to that for modeling fracture in homogeneous materials, and so we do not present many of the details provided in Dolbow (1999) and Moës et al. (1999).

The Galerkin approximation to the weak form (20) begins by considering a finite dimensional subspace $\mathscr{U}_0^h$ of $\mathscr{U}_0$ spanned by N linearly independent functions in $\mathscr{U}_0$. We then pose the weak form in $\mathscr{U}_0^h$ as follows:

$$\int_\Omega \boldsymbol{\epsilon}(\boldsymbol{u}^h) : \boldsymbol{C} : \boldsymbol{\epsilon}(\boldsymbol{v}^h) \, d\Omega = \int_{\Gamma_t} \bar{\boldsymbol{t}} \cdot \boldsymbol{v}^h \, d\Gamma \quad \forall \boldsymbol{v}^h \in \mathscr{U}_0^h \tag{21}$$

For the sake of concreteness, we now consider a rectangular domain Ω and a regular finite element triangulation $\mathscr{T}^h = \cup_{e=1}^{\text{nel}} \mathscr{T}_e$ such that $\mathscr{T}^h = \Omega$ as shown in Fig. 4. The characteristics of the FGM are modeled simply by taking the material properties at Gaussian integration points according to the functional form

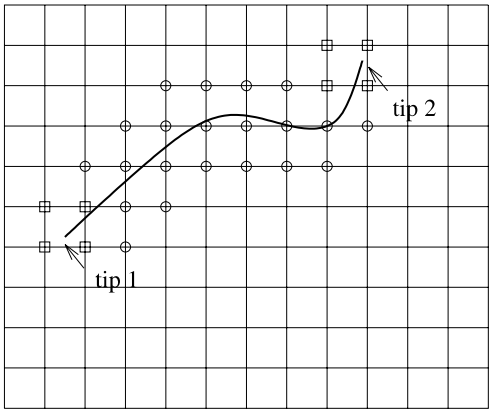

Fig. 4. An arbitrary crack placed on a mesh.

of $\boldsymbol{C}$. For accurate integration of the exponential fields examined in Section 4, a 4×4 quadrature rule is sufficient to bound the integration error below the approximation error.

Fig. 4 depicts a crack whose geometry Γ_c is taken to be independent of the mesh. A standard finite element basis for $\mathscr{U}_0^h$ is constructed from the space of complete polynomials $P^k(\mathscr{T}_e^h)$ of order $\leqslant k$ over each element:

$$\mathscr{U}_0^h = \operatorname{span}\{\phi_i\}_{i=1}^N \quad \text{where } \{\phi_i \in [C^0(\mathscr{T}^h)]^2 : \phi_i|\mathscr{T}_e^h \in [P^k(\mathscr{T}_e^h)]^2 \quad \text{and} \quad \phi_i|_{\Gamma_u} = 0\} \tag{22}$$

where the functions $\phi_i(\boldsymbol{x})$ are typically the nodal shape functions. Any linear combination of these functions results in a continuous interpolation for the displacement field, and furthermore possesses poor approximation properties for representing the singular stress fields near crack tips. Standard finite element approaches therefore construct "broken" meshes that conform to the crack geometry in order to represent the discontinuity, and employ significant mesh refinement or special singular elements near crack tips.

The X-FEM takes an alternative approach by *extending* the standard finite element approximation. We consider the set of overlapping subdomains defining the support of each nodal shape function and sets of enrichment functions $\{\mathscr{E}_i^k\}$ that possess desirable approximation properties over each subdomain. The method follows the *partition-of-unity* framework (Melenk and Babuška, 1996) through multiplying the enrichment functions by the nodal shape functions ϕ_i in order to ensure a conforming approximation. A general X-FEM basis for $\mathscr{U}_0^h$ is therefore

$$\mathscr{U}_0^h = \operatorname{span}\left\{ \{\phi_i\} \cup \{\phi_i \mathscr{E}_i^k\}_{k=1}^{n_i^E} \right\}_{i=1}^n \tag{23}$$

where n is the number of standard nodal shape functions and n_i^E is the number of enrichment functions for node i.

In practice, only those functions whose supports are in the vicinity of a feature of interest are enriched, giving the approximation a local character. For example, the X-FEM approximation for a crack is given by

$$\boldsymbol{u}^h(\boldsymbol{x}) = \sum_{i\in I} \boldsymbol{u}_i \phi_i(\boldsymbol{x}) + \sum_{l\in L} \boldsymbol{b}_l \phi_l(\boldsymbol{x}) H(\boldsymbol{x}) + \sum_{m\in M_1} \phi_m(\boldsymbol{x}) \left(\sum_{n=1}^4 \boldsymbol{c}_m^{n1} F_1^n(r,\theta) \right) + \sum_{m\in M_2} \phi_m(\boldsymbol{x}) \left(\sum_{n=1}^4 \boldsymbol{c}_m^{n2} F_2^n(r,\theta) \right) \tag{24}$$

where I is the set of all nodes in the mesh, L is the set of nodes enriched with the generalized Heaviside function $H(\boldsymbol{x})$, and (M_1, M_2) are the sets of nodes enriched with the sets of near-tip functions $F_1^n(r,\theta)$ and

$F_2^n(r,\theta)$ respectively. The set J is circled in Fig. 4 while the sets (M_1, M_2) are squared. A detailed definition of these sets, the criteria used to determine them numerically, and the construction of the enrichment functions is provided in Dolbow et al. (2000a). Importantly, enrichment with the function $H(\boldsymbol{x})$ allows for the representation of an arbitrary crack discontinuity while the sets of near-tip functions $F^n(r,\theta)$ capture the singular stress field.

Substitution of the approximation (24) into (21) and invoking the arbitrariness of the test functions results in a linear algebraic equation for these degrees of freedom:

$$\boldsymbol{K}\boldsymbol{d} = \boldsymbol{f} \tag{25}$$

where $\boldsymbol{K}$ is the elastic stiffness matrix and $\boldsymbol{f}$ is the vector of nodal forces. The vector of nodal unknowns $\boldsymbol{d}$ gathers the degrees of freedom $\{\boldsymbol{u}_i, \boldsymbol{b}_j, \boldsymbol{c}_k^{l1}, \boldsymbol{c}_k^{l2}\}$.

For the numerical evaluation of the domain integrals presented in the previous section, it is necessary to define a finite region A about the crack tip as well as a weight function q that vanishes on its boundary. In the present investigation, we first determine the characteristic length of an element touched by the crack tip and designate this quantity as h_{local}. For two dimensional analysis, this quantity is calculated as the square root of the element area. The domain A is then set to be all elements which have a node within a ball of radius r_{d} about the crack tip. The weight function q is taken to have a value of unity for all nodes within the ball r_{d}, and zero on the outer contour. The function is then easily interpolated within the elements using the nodal shape functions. Additional details are provided in Moës et al. (1999).

4. Numerical examples

In order to demonstrate the accuracy and utility of the domain form of the interaction energy integral, we present a few numerical examples in this section. We first consider the case of an edge cracked plate with a functional gradient in material properties. This problem has an analytical solution, and it is used to demonstrate the importance of retaining the inequality terms in the interaction energy integral. We then examine the case of a plate with an angled center crack and illustrate the effects of the functional gradient on the mixed-mode stress intensity factors.

4.1. Edge cracked plate

We consider a rectangular plate of width W and height $2h$ with an edge crack of length a subjected to a far-field stress σ^0 as shown in Fig. 5. The coordinate system is taken to coincide with the left hand side of the plate and the crack axis as shown. We assume that Poisson's ratio is a constant and that the spatial variation of Young's modulus is given by

$$E(x) = C_1 \, \mathrm{e}^{C_2 x} \tag{26}$$

where

$$C_1 = E_1, \quad C_2 = \ln(E_2/E_1)/W$$

The problem models an FGM whose properties transition from material 1 to material 2. The quantities E_1 and E_2 in Eq. (26) are the Young's moduli for the two different materials. Analytical solutions for the stress intensity factor K_1 for this problem as $h \to \infty$ were derived in Erdogan and Wu (1997). In order to approximate an infinite boundary, we set $h/W = 10$. In the following, all results are reported for a uniform mesh of 32×320 quadrilateral elements, and we did not find it necessary to apply symmetry conditions to reduce the computational cost. This discretization was found to yield results with less than a 1% difference to those obtained with a 16×160 mesh, and so the reported results represent converged solutions.

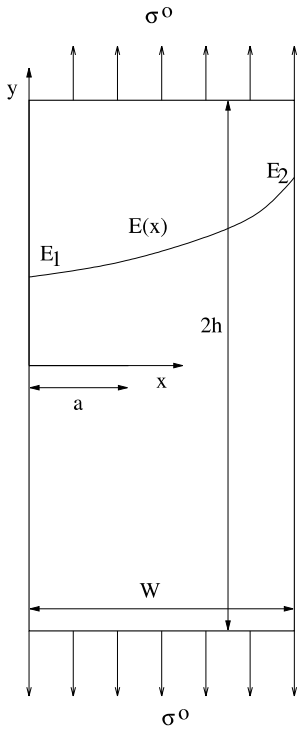

Fig. 5. Edge-cracked plate for the benchmark problems.

Stress intensity factors were calculated for crack lengths of $a/W = 0.2$ and 0.4 and various ratios (E_2/E_1). The results are summarized in Table 1. The table indicates a good comparison between the numerical and analytical results. The error ranges from 0.2% to 2.2% over all trials. Results are reported using a domain size generated from $r_d/h_{local} = 3.0$. These observations are consistent with the results reported in Anlas et al. (2000). We note that the error generally increases slightly as the Young's moduli for the two materials diverge, and is most likely the result of using a finite domain.

Using the same example problem, we now illustrate the domain-independence of the interaction energy integral and the importance of retaining the extra terms in the domain integrals that arise due to the lack of compatibility of the chosen auxiliary strain field. We repeat the calculations for the case when $E_2/E_1 = 10.0$ and for various ratios of r_d/h_{local}. The results are provided in Fig. 6. Under purely mode I loading, a simple relation exists between the J-integral and the stress intensity factor through (6):

$$K_I = \sqrt{E'_0 J} \tag{27}$$

Table 1
Normalized K_I values for various crack lengths and material properties

Crack length E_2/E_1	$a/W = 0.2$			$a/W = 0.4$		
	$K_I/\sigma^0\sqrt{\pi a}$	Analytical	Error (%)	$K_I/\sigma^0\sqrt{\pi a}$	Analytical	Error (%)
0.1	1.279	1.2965	1.3	2.552	2.570	0.7
0.2	1.381	1.396	1.1	2.438	2.443	0.2
1.0	1.363	1.373	0.7	2.116	2.107	0.4
5.0	1.133	1.132	0.09	1.752	1.748	0.2
10.0	1.004	1.024	2.0	1.590	1.626	2.2

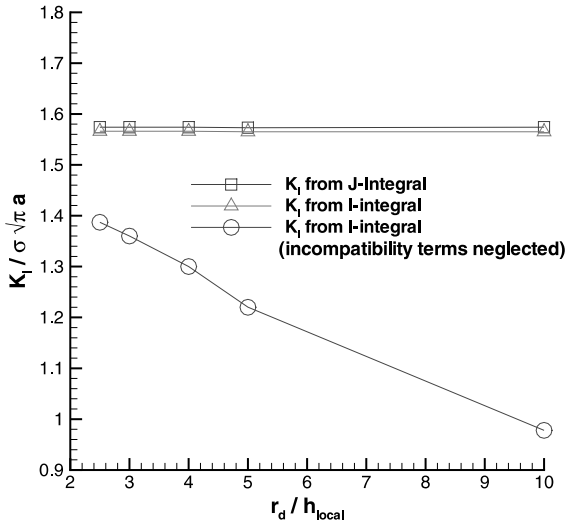

Fig. 6. Comparison of results for edge cracked plate with $E_2/E_1 = 10.0$ for different domain sizes.

The results clearly show good correlation between the domain forms of the J-integral (17) and the domain form of the interaction energy integral (16). The difference between these two numerical values is less than one percent in all cases tested. More importantly, the numerical results for both integrals exhibit domain independence. By way of contrast, the values obtained using the I integral when the incompatibility terms are neglected clearly exhibit domain dependence. Even for relatively small domains, the 11% error is significant for this latter case.

4.2. Edge crack with shear loading

In order to demonstrate our capabilities for a general case with mixed-mode stress intensity factors, we consider an edge cracked plate subjected to a shear load. We take the geometry shown in Fig. 5, with $2h/W = 16/7$, $a/W = 0.5$, the bottom surface clamped and the top subjected to a positive shear traction τ^0. The Young's modulus is again taken to be variable with position as given by (26). All of the results reported in this section were obtained using a uniform partition of 48×96 quadrilateral elements. The results obtained with this level of discretization were found to be within 1% of the results obtained with a 24×48 mesh, and therefore represent converged quantities.

We note that for the four-point bending specimens examined by Gu and Asaro (1997), the second integral in (16) would vanish as the crack tip is oriented perpendicular to the gradient in Young's modulus. The problem examined here therefore represents a more general case of mixed-mode loading, and should serve as a benchmark for future investigations into the mixed-mode fracture of FGMs.

For uniform material properties ($E_2 = E_1$), the exact stress intensity factors are given by Yau et al. (1980). While the geometry and loading is fairly simple, to our knowledge an analytical solution does not exist for the functionally graded case. The numerical results shown in Fig. 7 are normalized by the exact solution for homogeneous material properties. We recover the exact solution to within 1% for the homogeneous case. We also observe a decrease in both K_{I} and K_{II} as the ratio E_2/E_1 increases, which is consistent with the results reported in Table 1.

Of further interest to crack propagation analysis is the influence of the material gradients on the phase angle,

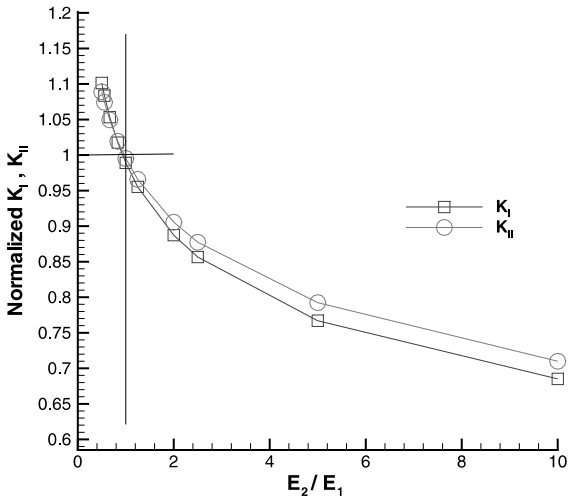

Fig. 7. Stress intensity factors for edge crack with shear load and functionally graded Young's modulus E. The values have been normalized by the exact solution for a uniform E.

$$\psi = \tan^{-1} \frac{K_{\mathrm{II}}}{K_{\mathrm{I}}} \tag{28}$$

as it indicates the degree of mode-mixity at the crack tip. The variation in this quantity for the present case is illustrated in Fig. 8, with results again normalized by the homogeneous value of 7.62°. We note from this plot and the results reported in Fig. 7, that while both K_{I} and K_{II} vary by $\approx$40% over the range of (E_2/E_1) considered, the phase angle varies by $<$5%.

As an additional check on the present numerical results, we also compute the energy release rate by evaluating the domain representation of the J-integral (17) and comparing its value to that obtained by calculating (6) using K_{I} and K_{II} obtained from the domain form of the interaction energy integral (16). The results are provided in Table 2, and indicate that these two values are within 1% for all cases tested.

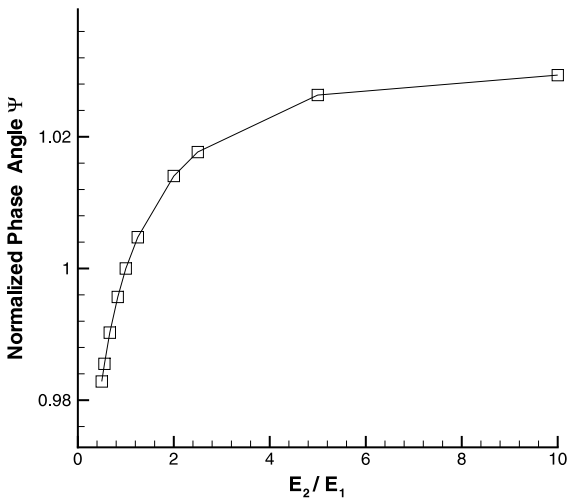

Fig. 8. Phase angle for edge crack with shear load and functionally graded Young's modulus E.

Table 2
Normalized results for edge-cracked plate subjected to shear traction

E_2/E_1	K_I	K_{II}	$E_0'G/(K_I^2+K_{II}^2)$
0.5	1.110	1.093	1.004
0.556	1.092	1.078	1.004
0.667	1.061	1.052	1.004
0.833	1.016	1.014	1.003
1.0	0.996	0.997	1.004
1.25	0.962	0.967	1.004
2.0	0.893	0.905	1.004
2.5	0.862	0.877	1.004
5.0	0.772	0.791	1.004
10.0	0.689	0.708	1.004

4.3. Plate with angled center crack

As a last example, stress intensity factors are calculated for the problem of a square plate with an angled center crack as shown in Fig. 9. The plate is subjected to a far-field state of stress σ_{yy}, and K_I and K_{II} are obtained as a function of the crack angle β. In this example, the plate dimensions are chosen to be $W = 20.0$ in. The half crack length is taken to be $a = 1.0$ in., and the same mesh of 60×60 quadrilateral elements is used for all calculations. This level of discretization was found to yield a converged solution (results were within 1% of those for a 120×120 grid).

In order to facilitate comparison with the analytical solution of Konda and Erdogan (1994), we take Young's modulus to vary exponentially as

$$E(x) = E_0\, e^{\alpha x} \tag{29}$$

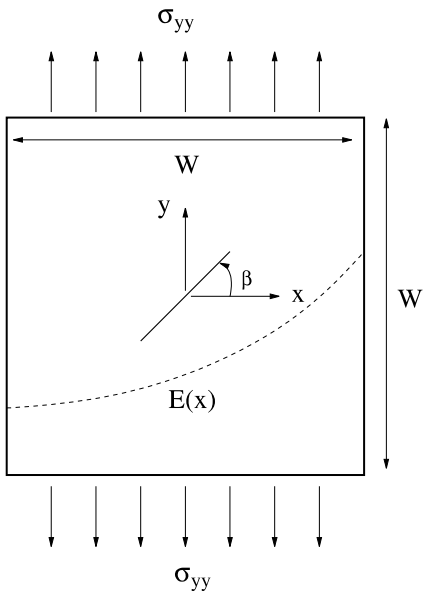

Fig. 9. Square plate with angled center crack and functionally graded Young's modulus $E(x)$. Results for both varying and constant far-field stress σ_{yy} are presented.

Table 3
Comparison of numerical and analytical stress intensity factors for plate with angled center crack, exponentially varying Young's modulus, and $\sigma_{yy} = E_0 e^{\alpha x}$

β/π	$K_I(a)/\sqrt{\pi a}$	Analytical	$K_I(-a)/\sigma^0\sqrt{\pi a}$	Analytical	$K_{II}(a)/\sqrt{\pi a}$	Analytical	$K_{II}(-a)/\sqrt{\pi a}$	Analytical
$\alpha a = 0.25$								
−0.0	1.218	1.196	0.838	0.825	0.000	0.0	0.000	0.0
−0.1	1.099	1.081	0.761	0.750	−0.329	−0.321	−0.257	−0.254
−0.2	0.788	0.781	0.557	0.548	−0.524	−0.514	−0.424	−0.422
−0.3	0.415	0.414	0.295	0.290	−0.512	−0.504	−0.439	−0.437
−0.4	0.118	0.121	0.077	0.075	−0.306	−0.304	−0.282	−0.282
−0.5	0.000	0.0	0.000	0.0	0.000	0.0	0.000	0.0
$\alpha a = 0.50$								
−0.0	1.445	1.424	0.681	0.674	0.000	0.0	0.000	0.0
−0.1	1.303	1.285	0.623	0.617	−0.353	−0.344	−0.213	−0.213
−0.2	0.930	0.925	0.467	0.460	−0.560	−0.548	−0.364	−0.365
−0.3	0.488	0.490	0.251	0.247	−0.540	−0.532	−0.396	−0.397
−0.4	0.142	0.146	0.062	0.059	−0.316	−0.314	−0.268	−0.269
−0.5	0.000	0.0	0.000	0.0	0.000	0.0	0.000	0.000

where E_0 is the modulus at the center of the crack. Poisson's ratio is held fixed at 0.3, and we take $E_0 = 1.0$ Pa for the sake of simplicity.

We begin by examining the case where the applied stress also varies spatially as the above equation, representing the case of a uniform applied strain at the boundary of the specimen. A comparison of the numerical results to the analytical solution presented in Konda and Erdogan (1994) is provided in Table 3 for $\alpha a = 0.25$ and 0.5. Results for both stress intensity factors at both crack tips are reported for various angles β/π. We remark that we have adopted the opposite convention from the above reference of measuring the angle between the crack and material gradient. We observe excellent qualitative and quantitative agreement between the numerical and analytical results provided in Table 6 of Konda and Erdogan (1994). The error in the calculations ranges between less than 1% and 2%. The only exception is a 5% error for the value of $K_I(-a)$ for $\alpha a = 0.5$ and $\beta/\pi = 0.4$, but we note that both values are close to zero. The numerical values appear to be more accurate than those reported in Kim and Paulino (2002), though this may be attributable to the use of more total degrees of freedom in the present investigation. We also note that for all crack orientations, the energy release rate calculated from the stress intensity factors through (6) was found to be in excellent agreement with the measure of the domain form of the J-integral.

In the following, we also compare the numerical results to those for an infinite homogeneous plate subjected to a *uniform* far-field stress, $\sigma_{yy} = \sigma$. The analytical solution for the stress intensity factors is given by

$$K_I = \sigma\sqrt{\pi a}\cos^2(\beta) \tag{30}$$

$$K_{II} = \sigma\sqrt{\pi a}\sin(\beta)\cos(\beta) \tag{31}$$

The results for K_I as a function of β are reported for three different values of αa in Fig. 10. Analogous results for K_{II} are shown in Fig. 11. In both plots, results are reported for the rightmost crack tip when $\beta = 0$, and K_I and K_{II} are normalized by $\sigma\sqrt{\pi a}$.

The numerical results exhibit some interesting features. Excellent accuracy is obtained for the homogeneous case, with errors less than a few percent. We note that an increase in α leads to an increase in the mode I stress intensity factors at both crack tips. For the mode II stress intensity factors, our results indicate that K_{II} decreases with increasing material gradient, but the change from the homogeneous case is much less significant. We also note that when $\beta = 90°$, the crack is oriented parallel to the far-field traction,

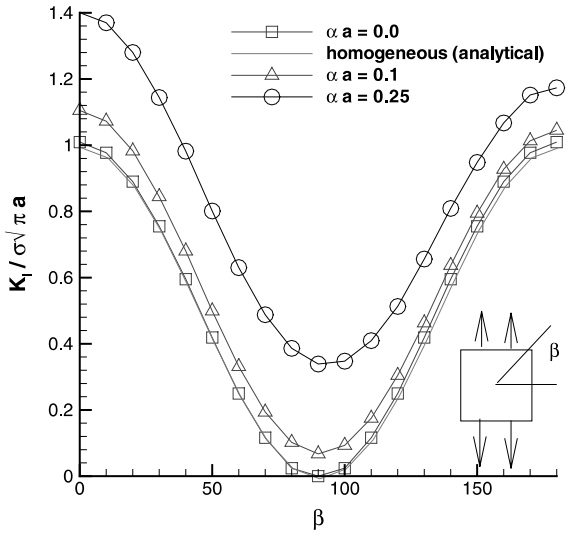

Fig. 10. Normalized mode I stress intensity factor for angled center crack subjected to far-field stress $\sigma_{yy} = \sigma$ for various gradients αa.

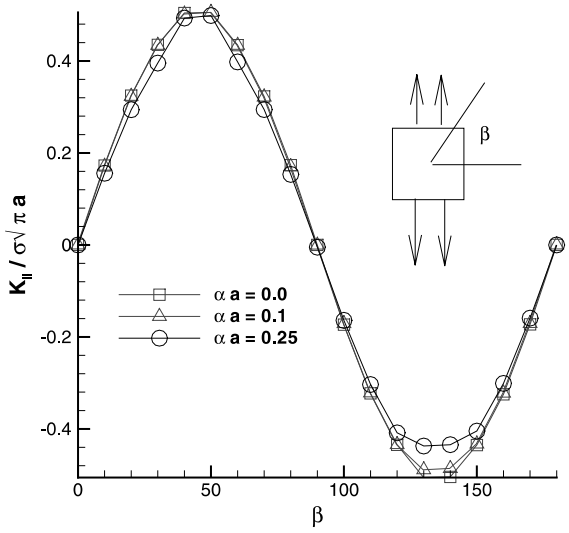

Fig. 11. Normalized mode II stress intensity factor for angled center crack.

and the gradients in material properties result in non-zero values for both K_{I} and K_{II}. This is in marked contrast to the results for the uniform strain case presented in Table 3.

5. Summary and concluding remarks

In the present paper, domain representations of interaction energy integrals were derived for evaluating mixed-mode stress intensity factors at the tips of arbitrarily oriented cracks in FGMs. The approach is

applicable to the analysis of any FGM in which the form of the asymptotic near-tip fields match those of a homogeneous material, and it does not require a detailed knowledge of the higher order terms. In the derivation, an interaction energy contour integral was expressed in domain form and evaluated as a post-processing step in the X-FEM. A key step in the derivation concerned the choice of auxiliary fields used to separate mixed-mode stress intensity factors. We examined several different possible choices for the auxiliary fields and the associated consequences of incompatibilities in the resulting domain integrals. We argued that a suitable choice is a solution consisting of the asymptotic stress and displacement fields, with an incompatible strain field that satisfies the constitutive relationships. In the domain integrals, these incompatibilities and the gradients in material properties give rise to additional terms which vanish for homogeneous materials.

In the numerical examples, excellent agreement between the numerical and analytical solutions was obtained for the edge-cracked plate problem. Domain independence was observed for all cases considered. Importantly, the results were in significant error when the incompatibility terms were ignored in the evaluation of the domain integrals. For the more general example with mixed-mode loading, the calculations of the energy release rate using the interaction energy integral yielded consistent results with the domain form of the J-integral. Gradients in material properties significantly affected both K_{I} and K_{II}, but the phase angle was relatively unchanged. Finally, the last example of a center cracked plate provided results that were in excellent agreement with published theoretical values.

We emphasize that much of the work presented in the paper was motivated by the need to numerically simulate crack propagation in FGMs. This stipulation is of course limited to analyses where crack growth can be reliably predicted from the interpretation of K_{I} and K_{II}. A robust and efficient numerical simulation of crack growth in FGMs requires a method to determine mixed-mode stress intensity factors without concern for domain dependence or sensitivity, and which preferably does not require user intervention. The formulation presented herein satisfies all of these requirements. It is also worth pointing out that the present approach may provide a means to investigate crack growth along bimaterial interfaces. Many such interfaces are not "true" interfaces, i.e. due to the chemical bonding procedure employed during fabrication, the interface may more closely resemble a thin layer across which the material gradients are rather steep. The present approach can certainly be used to investigate crack growth in this thin region. We note, however, that in the limit as the layer vanishes and a true bimaterial interface exists, the present approach is not valid because the material properties at the crack tip are not single-valued. In addition to crack growth studies, future work will focus on extending the present approach to problems involving FGMs subjected to thermal loading.

All of the post-processing routines employed for the calculation of the interaction energy integral are available at: http://ceelab4.egr.duke.edu/~dolbow/FGM/interact.html

Acknowledgements

The authors are grateful to Professor J.C. Nadeau, of Duke University, for several helpful comments during the preparation of this manuscript. The first author would also like to thank Professor Glaucio Paulino, of the University of Illinois, for directing him to his recent article on this topic.

References

Anlas, G., Santare, M., Lambros, J., 2000. Numerical calculation of stress intensity factors in functionally graded materials. International Journal of Fracture 104, 131–143.

Dolbow, J., 1999. An extended finite element method with discontinuous enrichment for applied mechanics. Ph.D. Thesis, Northwestern University.

Dolbow, J., Moës, N., Belytschko, T., 2000a. Discontinuous enrichment in finite elements with a partition of unity method. Finite Elements in Analysis and Design 36, 235–260.

Dolbow, J., Moës, N., Belytschko, T., 2000b. Modeling fracture in Mindlin–Reissner plates with the extended finite element method. International Journal of Solids and Structures 37, 7161–7183.

Eischen, J., 1983. Fracture of nonhomogeneous materials. International Journal of Fracture 34, 3–22.

Erdogan, F., 1995. Fracture mechanics of functionally graded materials. Composites Engineering 5 (7), 753–770.

Erdogan, F., Wu, B., 1997. The surface crack problem for a plate with functionally graded properties. ASME Journal of Applied Mechanics 61, 449–456.

Eshelby, J., 1956. The continuum theory of lattice defects. In: Seitz, F., Turnbull, D. (Eds.), Solid State Physics, vol. 3. Academic Press, New York, pp. 79–141.

Gosz, M., Dolbow, J., Moran, B., 1998. Domain integral formulation for stress intensity factor computation along curved three-dimensional interface cracks. International Journal of Solids and Structures 35, 1763–1783.

Gu, P., Asaro, R., 1997. Cracks in functionally graded materials. International Journal of Solids and Structures 34, 1–17.

Gu, P., Dao, M., Asaro, R., 1999. A simplified method for calculating the crack-tip field of functionally graded materials using the domain integral. Journal of Applied Mechanics 66, 101–108.

Honein, T., Herrmann, G., 1997. Conservation laws in nonhomogeneous plane elastostatics. Journal of the Mechanics and Physics of Solids 45 (5), 789–805.

Kim, J., Paulino, G., 2002. Finite element evaluation of mixed-mode stress intensity factors in functionally graded materials. International Journal for Numerical Methods in Engineering 53, 1903–1935.

Konda, N., Erdogan, F., 1994. The mixed mode crack problem in a nonhomogeneous elastic medium. Engineering Fracture Mechanics 47, 533–545.

Melenk, J.M., Babuška, I., 1996. The partition of unity finite element method: Basic theory and applications. Computer Methods in Applied Mechanics and Engineering 139, 289–314.

Moës, N., Dolbow, J., Belytschko, T., 1999. A finite element method for crack growth without remeshing. International Journal for Numerical Methods in Engineering 46, 131–150.

Nadeau, J., Ferrari, M., 1999. Microstructural optimization of a functionally graded transversely isotropic layer. Mechanics of Materials 31, 637–651.

Nahta, R., Moran, B., 1993. Domain integrals for axisymmetric interface crack problems. International Journal of Solids and Structures 30 (15), 2027–2040.

Nakamura, T., 1991. Three-dimensional stress fields of elastic interface cracks. Journal of Applied Mechanics 58, 939–946.

Rice, J., 1968. A path independent integral and the approximate analysis of strain concentration by notches and cracks. ASME Journal of Applied Mechanics 35, 379–386.

Shih, C., Moran, B., Nakamura, T., 1986. Energy release rate along a three-dimensional crack front in a thermally stressed body. International Journal of Fracture 30, 79–102.

Takahashi, H., Ishikawa, T., Okugawa, D., Hashida, T., 1993. Laser and plasma-arc thermal shock/fatigue fracture evaluation procedure for functionally gradient materials. In: Schneider, G., Petzow, G. (Eds.), Thermal Shock and Thermal Fatigue Behavior of Advanced Ceramics. Kluwer Academic Publishers, Dordrecht, pp. 543–554.

Yau, J., Wang, S., Corten, H., 1980. A mixed-mode crack analysis of isotropic solids using conservation laws of elasticity. Journal of Applied Mechanics 47, 335–341.